

Cambridge University Press

0521810590 - Imaging in Molecular Dynamics: Technology and Applications

Edited by Benjamin J. Whitaker

Excerpt

[More information](#)

## Part One

### Technology

# 1

## Charged particle imaging in chemical dynamics: an historical perspective

PAUL L. HOUSTON

### 1.1 Introduction

Many problems in molecular dynamics demand the simultaneous measurement of a particle's speed and angular direction; the most demanding require the measurement of this velocity in coincidence with internal energy. Studies of molecular reactions, energy transfer processes, and photodissociation events can be understood completely only if the internal energies and velocities of all products are specified.

Consider the case of a monochromatic photodissociation that produces two fragments A and B. Even if the internal energy distributions of A and B were each measured separately, it would still be necessary to obtain information on their recoil speed in order to determine the internal *energy* of B given a selected level of A. Measurement of the coincident *level* of B would further require that only one parent molecule be dissociated in any particular experiment – a true coincidence experiment. Angular information is also desirable. In photodissociations, for example, the recoil angle with respect to the polarization vector of the dissociating light provides information about the transition moment in the parent molecule and the time-scale of dissociation. Because reactions in molecular beams have many of these same requirements, new techniques for simultaneous measurement of velocity and internal energy are quite important to molecular dynamics.

Many of the current techniques for making simultaneous velocity and internal energy measurements are based on imaging of product molecules or particles with microchannel plate (MCP) detectors. This introductory chapter traces the development of charged particle imaging techniques in molecular dynamics with emphasis on the early ideas that influenced the field. Any such history is, of course, personal and incomplete. This one is no exception. The attempt made here is to provide the background for the exciting work on photodissociation, photoionization,

and bimolecular processes using both noncoincidence and coincidence techniques reported in this monograph.

### 1.2 The need for angular information: vector correlations

From the very beginning of the field of molecular dynamics, angular information has been recognized as essential to the understanding of crossed molecular beam reactions [1]. However, the angular information in photodissociation and photoionization processes has only more recently become of interest. Herschbach and Zare first pointed out that the vector correlation between the parent's transition dipole moment,  $\mu$ , and the velocity of the product,  $v$ , can lead to an anisotropic distribution of photofragments [2]. Photolysis light with a linear polarization defined in the laboratory frame will preferentially excite those parent molecules whose dipole transition moments are aligned parallel to the electric vector of the dissociating light. In the molecular frame, it is nearly always the case that the direction of fragment departure, which defines the recoil velocity vector  $v$ , has a fixed angular relationship to  $\mu$ ; for example, in a diatomic parent molecule,  $v$  will be either parallel or perpendicular to  $\mu$ . Consequently, if  $\mu$  is aligned in the laboratory frame by the dissociating light,  $v$  will also be aligned in the laboratory frame, provided that the dissociation takes place rapidly enough so that the alignment of  $\mu$  is not lost before the moment of fragmentation.

Zare noted that the normalized angular distribution of photofragments should be given by the equation [3]

$$I(\vartheta) = (4\pi)^{-1}[1 + \beta P_2(\cos \vartheta)], \quad (1.1)$$

where  $\vartheta$  is the angle between  $v$  and the electric vector of the dissociating light,  $P_2(\cos \vartheta)$  is the second Legendre polynomial, and  $\beta$  is a parameter that describes the degree of anisotropy ( $-1 \leq \beta \leq 2$ ). Since the dissociation light aligns the transition dipole moment  $\mu$  in the laboratory frame, and since for a diatomic molecule  $\mu$  is either parallel or perpendicular to  $v$ , measurement of  $v$  in the laboratory frame can be used to determine the molecular-frame alignment of  $\mu$ . Thus, for rapid dissociations of a diatomic molecule, an anisotropy parameter of  $\beta = 2$ , giving a distribution  $I(\vartheta) \propto \cos^2 \vartheta$ , would indicate that  $\mu$  is parallel to the breaking bond, while a parameter of  $\beta = -1$ , giving a distribution of  $I(\vartheta) \propto \sin^2 \vartheta$ , would indicate that  $\mu$  is perpendicular to the breaking bond. For polyatomic molecules the situation is somewhat more complicated. If one assumes the rapid dissociation limit then  $\beta = 2P_2(\cos\alpha)$ , where  $\alpha$  is the angle between  $\mu$  and the breaking bond.

Solomon was the first to observe an anisotropic distribution of photofragment recoil velocities [4]. Linearly polarized visible light was used to photolyze bromine or iodine within a hemispheric bulb whose inside surface had been coated with a

## Charged particle imaging: an historical perspective

5

thin film of tellurium. The pressure of the parent gas was held low enough so that the mean free path of the atomic fragments was larger than the radius of the bulb. The etching rate of the tellurium film as the atoms recoiled to the surface of the bulb was observed to depend on the angle between the velocity and the electric vector of the dissociating light. In both cases, the flux of dissociated atoms peaked perpendicular to the electric vector of the photolysis light, and the experiment was interpreted as indicative of a ‘perpendicular’ transition with  $\beta = -1$ . This ‘photolysis mapping’ method was later used by Solomon *et al.* to investigate the dissociations of aliphatic carbonyl compounds [5]. It was clear, however, that new methods would be needed.

A more quantitative method for measuring recoil velocity distributions was developed in 1969 almost simultaneously by Busch *et al.* [6] and by Diesen *et al.* [7]. In these experiments, a linearly polarized ruby laser was used to dissociate a halogen or interhalogen molecule, while a quadrupole mass spectrometer was employed to detect the arrival time and angular distributions of atomic fragments. A schematic diagram of the apparatus is shown in Fig. 1.1. The principal advantage of this detection technique was that both the direction and magnitude of the recoil velocity could be determined. In the case of  $I_2$ , for example, two peaks in the arrival time were observed, corresponding to the two accessible spin-orbit states of the I atom. Even

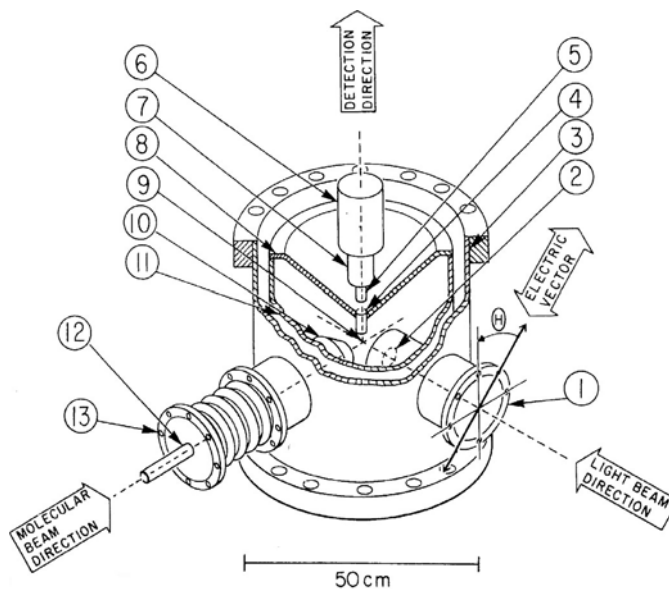


Fig. 1.1. Schematic diagram of photofragment spectrometer. (1) laser beam port, (2) lens, (3) chamber, (4) collimating tube, (5) ionizer, (6) electron multiplier, (7) quadrupole mass spectrometer, (8) partition, (9) interaction volume, (10) collimator, (11) inner wall, (12) molecular beam, (13) molecular beam port. Reprinted with permission from Ref. [8]. Copyright 1972, American Institute of Physics.

though this technique was a great advancement, it did not yet allow determination of the velocity distribution of a *state-selected* product.

### 1.3 The Doppler effect

Johann Christian Doppler was born in Salzburg in 1803. The effect that bears his name is familiar to all: the frequency of a sound wave heard by an observer depends on the relative speed between the observer and the source of the sound. It was actually Armand Fizeau in 1848 who pointed out that the same effect occurred for light waves. Specifically, the frequency of light absorbed by a moving object is shifted by an amount that depends on the relative velocity between the light source and the object:  $v_{\text{abs}} = v_0[1 - (v/c)]$ , where  $v_0$  is the frequency that would be absorbed in the absence of relative motion,  $v$  is the relative velocity, and  $c$  is the speed of light. Thus, if a molecule to be probed by an absorption-based technique is moving toward the light source, it will absorb at a slightly lower frequency than if it is moving away from the laser. The distribution of absorption frequencies is thus directly related to the distribution of molecular speeds.

The Doppler profile of an absorption can be viewed in a suggestive way: it is simply the projection of the three-dimensional velocity distribution for the probed product onto one dimension, that is, onto the line describing the propagation direction of the probe light. It is well known from spectral broadening studies at low pressure that molecules having a Maxwellian distribution of speeds display a Gaussian spectral line shape whose half-width is proportional to the square root of the temperature. It is less well known that an ensemble of molecules having velocities isotropic in space but characterized by a single speed  $v$  exhibits a Doppler profile of equal absorption intensity throughout the line but with sharp edges at frequencies  $v = v_0[1 \pm (v/c)]$ . For an arbitrary distribution of speeds, but still for an isotropic distribution in space, the speed distribution  $P(v)$  is simply proportional to the derivative of the Doppler profile at the frequency  $v$  corresponding to the velocity  $v$ . Although the relationship is less simple if the velocity distribution is not isotropic or if there are angular relationships between the velocity vector and the angular momentum vector [9], even in these cases multiple measurements of the Doppler profile using different detection geometries or different spectral transitions can lead unambiguously to the distribution of speeds. Kinsey demonstrated [10] that the full three-dimensional velocity distribution can be reconstructed by a Fourier transform technique from Doppler profiles measured at several different angles.

From the point of molecular dynamics, use of the Doppler technique had, however, another powerful advantage, state selectivity. Two of the most sensitive laser-based detection techniques are laser-induced fluorescence (LIF) and

*Charged particle imaging: an historical perspective*

7

resonance-enhanced multiphoton ionization (REMPI). Both depend on absorption, and both can be used to detect a product in a single spectroscopic state. By measuring the Doppler profile of products detected by one of these techniques, researchers could finally determine the velocity distribution of a state-selected species. We consider a few important early examples.

Schmiedl *et al.* monitored the Doppler profile of the ground-state H atom produced in the 266-nm dissociation of HI by using vacuum-ultraviolet laser-induced fluorescence [11]. For a fragment whose speed distribution is given measured in the direction  $\mathbf{k}$  making an angle  $\vartheta'$  with respect to the electric vector of the (linearly polarized) dissociation light, then it can be shown that the Doppler profile for laser-induced fluorescence is given by [11]

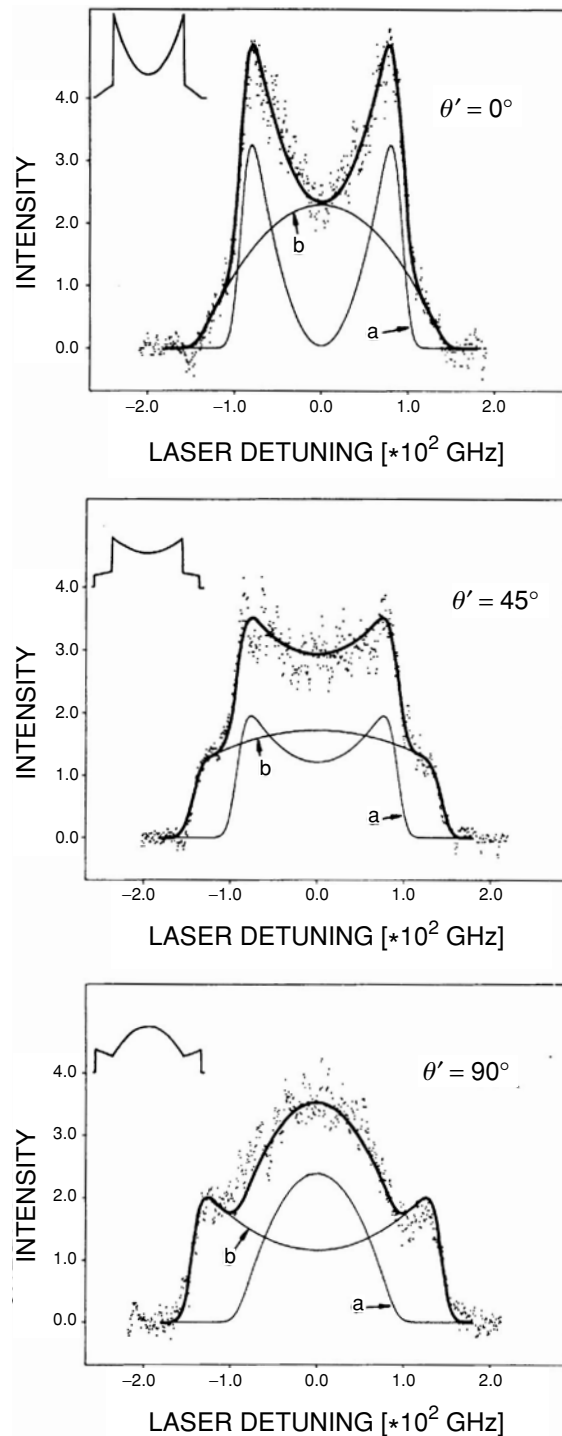
$$I(\chi) = (4\pi)^{-1} [1 + \beta P_2(\cos \vartheta') P_2(\cos \chi)], \quad (1.2)$$

where  $v_0 \cos \chi$  is the Doppler shift.

Figure 1.2 displays Doppler profiles observed by Schmiedl *et al.* [11] in the 266-nm dissociation of HI for angles  $\vartheta' = 0^\circ, 45^\circ$  and  $90^\circ$ . For photolysis at this wavelength there are two dissociative channels, one producing  $\text{H} + \text{I}({}^2\text{P}_{1/2})$  via a  $\Delta\Omega = 0$  (parallel) transition and another producing  $\text{H} + \text{I}({}^2\text{P}_{3/2})$  via a  $\Delta\Omega = 1$  (perpendicular) transition. Thus, since the former channel deposits more energy into internal degrees of freedom, we expect to observe a profile composed of slower fragments recoiling with a distribution characteristic of a parallel transition ( $\beta = 2$ ) and faster fragments recoiling with a distribution characteristic of a perpendicular transition ( $\beta = -1$ ). Composite profiles based on (1.2) do indeed fit the data, as shown by the sum of curves a and b in Fig. 1.2.

Another example illustrates the use of the Doppler effect for studies of differential cross-sections in crossed beam collisions. In this experiment, a beam  $\text{Na}(3\ {}^2\text{P}_{1/2})$  was prepared by laser excitation and crossed with a beam of argon atoms [12]. Fine structure changing collisions created  $\text{Na}(3\ {}^2\text{P}_{3/2})$ , which was probed by laser excitation with sub-Doppler resolution. Figure 1.3 shows the principle of the technique. The scattered products of the reaction are cylindrically symmetric about the relative velocity vector for the collision and are scattered at an angle  $\vartheta$  with respect to the original direction of the sodium. By choosing the propagation direction of the probe laser to be parallel to the relative velocity vector for the collision, the authors were able to directly map the differential cross-section as a function of the projection  $\cos \vartheta$  on to the Doppler profile, also a function of  $\cos \vartheta$ . The cross-sections obtained were in quite reasonable agreement with those predicted by theory [13].

A third important early example is the study of the photodissociation of ICN by Nadler *et al.* [14]. These authors used sub-Doppler laser-induced fluorescence to measure the velocity of individual CN internal energy levels. Because more recoil



## Charged particle imaging: an historical perspective

9

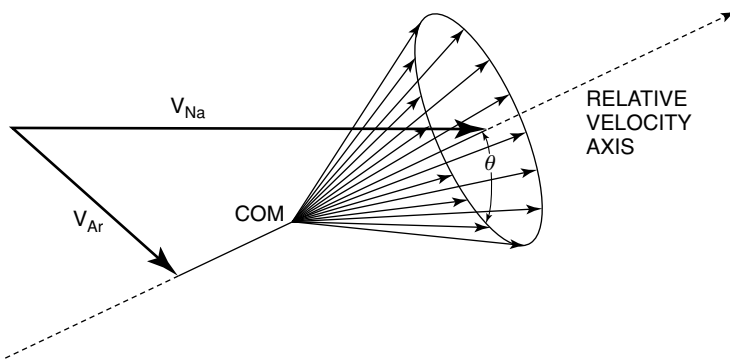


Fig. 1.3. Velocity vector diagram. Bold vectors are initial beam velocities, while light vectors are scattered Na velocities in the center-of-mass frame for scattering through angle  $\vartheta$  for different values of  $\phi$ . Reprinted with permission from Ref. [12]. Copyright 1978, American Physical Society.

energy is available if the iodine product is produced in the  $I(^2P_{3/2})$  ground state than if it is produced in the  $I(^2P_{1/2})$  excited state, most Doppler profiles consisted of two components. By resolving these velocity components, the authors were able to determine that high rotational levels of CN were produced in coincidence with ground-state iodine atoms, while low rotational levels are produced in coincidence with excited-state iodine atoms.

The use of a Wiley–McLaren time-of-flight (TOF) spectrometer is an alternative method for making a one-dimensional projection that leads us somewhat closer to charged particle imaging. In an early example, Ogorzalek *et al.* [15, 16] photodissociated  $CD_3I$  at 266 nm and ionized the  $I(^2P_{1/2})$ ,  $I(^2P_{3/2})$ , or  $CD_3(v, J)$  products using a second laser. By delaying the pulsed voltage on the repeller and extraction grid, they were able to stretch out the arrival time of the appropriate mass peak. The peaks reveal structure due to the recoil velocity of the  $I$ ,  $I^*$ , or  $CD_3$  fragments in just the same way as does a Doppler profile, because products moving originally toward or away from the detector arrive at differing time delays. A variant on the technique sampled a one-dimensional core through the three-dimensional distribution [16]. Ogorzalek *et al.* were able to measure the anisotropic angular distributions of the

Fig. 1.2. (Left) Experimental Doppler line profiled (dots) measured at probe angles  $\vartheta' = 0^\circ$ ,  $45^\circ$  and  $90^\circ$ , where  $\vartheta'$  is the angle between the electric vector of the photolysis light and the propagation direction of the probe light. The theoretical profiles (a) and (b) are for pure parallel ( $\beta = 2$ ) and perpendicular ( $\beta = -1$ ) transitions, weighted such that superposition yields the best fits to the experimental profiles (heavy curves). Inserted in the top left corners are illustrations of the theoretical sum profiles expected under ideal resolution. Reprinted with permission from Ref. [11]. Copyright 1982, Springer-Verlag.

I or CD<sub>3</sub> products and to correlate I/I\* distributions with CD<sub>3</sub> vibrational level. It may have first been a suggestive remark by Ara Apkarian during these experiments that started our own group thinking of how it might be nice to combine the TOF mass spectrometric technique with two-dimensional detection.

In addition to providing correlated information on the products of photodissociation, the one-dimensional velocity projection afforded by the Doppler effect or by TOF mass spectrometry had another important advantage: the measurement was multiplexed in the sense that the velocity of every fragment contributed to some part of the signal. On the other hand, noise on the Doppler profile tended to be amplified in the deconvolution, so that it was sometimes difficult to obtain accurate data. A very reasonable extension of the technique was to make a two-dimensional projection. Fortunately, in the mid-1980s microchannel plate detectors and charge-coupled device (CCD) cameras were just becoming affordable.

#### 1.4 The ESDIAD inspiration

Much of the inspiration for attempting a two-dimensional projection of reaction products came from work in a different area of investigation, surface science. In 1974, Yates and his colleagues first introduced the technique of electron stimulated desorption ion angular distributions (ESDIAD) [17]. These authors discovered that the direction of ions emitted when a surface layer is desorbed by electron bombardment depends on the alignment of the surface layer with respect to the underlying surface. They were able to detect the desorption direction by accelerating the ions with a hemispherical grid into a microchannel plate assembly. Electrons produced in the microchannel plates were further accelerated to a screen and the resulting image was photographed.

A recent example of the sort of results that can be obtained with this technique is shown in Fig. 1.4, which illustrates the results of a study of the rotation of the deuterated methyl group in methyl acetate adsorbed on a Cu(110) surface. At low temperatures, a four-peak pattern is observed that corresponds to a non-rotating methyl group oriented parallel or antiparallel to a particular axis of the copper and having one D atom pointing toward the surface. At higher temperatures, the methyl group rotates freely, and a circular pattern is observed. By fitting patterns at different temperatures to a linear combination of the four-peak and the circular pattern, the authors were able to measure the amount of rotation as a function of temperature, from which they deduced that the barrier height to rotation was 7 ± 4 meV for CD<sub>3</sub> and 12 ± 6 meV for CH<sub>3</sub>. The power of images such as these to convey important structural information was an important inspiration leading to the use of similar techniques in product imaging.

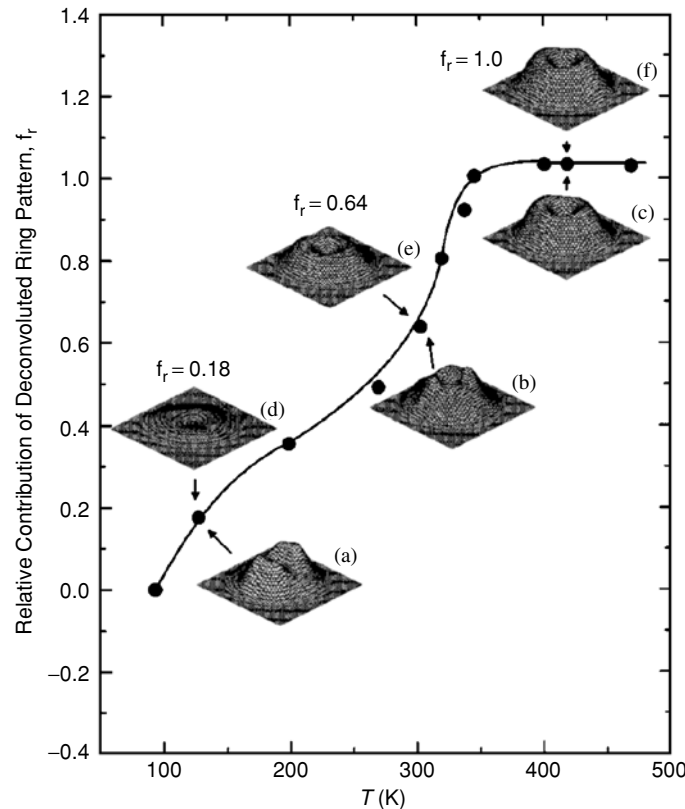


Fig. 1.4. Temperature dependence of the rotation of the methyl group of  $\text{CD}_3\text{COO}$ . Twofold symmetrized D + ESDIAD pattern for acetate/Cu(110) at high coverage. The (a), (b) and (c) patterns are the observed patterns at each temperature. The intensity of the (d), (e) and (f) patterns represent how much the ring pattern contributes in the observed patterns at each temperature. Reprinted from Ref. [18]. Copyright 2000, American Institute of Physics.

### 1.5 Product imaging

The stage was now set for the development of product imaging. As Dave Chandler remembers it, the idea of combining TOF mass spectrometry with microchannel plate detection of the products came to him while listening to a talk I gave about the experiments of Ogorzalek and Haerri at a November, 1986 Faraday Discussion in Bristol on the dynamics of photofragmentation. Dave actually sketched out an apparatus in his notebook and showed it to me after the talk. I indicated that we had thought somewhat about a two-dimensional projection, but that we certainly didn't have the resources to pursue it. Dave had access to a spare ESDIAD detector, so he proposed that I spend some time at Sandia trying to make a system work. My own recollection is that many of the details of the plan were worked out over beer that